Electrical Detection of Coherent Nuclear Spin Oscillations in Phosphorus-Doped Silicon using Pulsed ENDOR

Felix Hoehne,[1,*] Lukas Dreher,[1,†] Hans Huebl,[2] Martin Stutzmann,[1] and Martin S. Brandt[1]
[1]Walter Schottky Institut, Technische Universität München, Am Coulombwall 4, 85748 Garching, Germany
[2]Walther-Meißner-Institut, Bayerische Akademie der Wissenschaften, Walther-Meißner-Straße 8, 85748 Garching, Germany
(Received 23 December 2010; published 3 May 2011)

We demonstrate the electrical detection of pulsed X-band electron nuclear double resonance (ENDOR) in phosphorus-doped silicon at 5 K. A pulse sequence analogous to Davies ENDOR in conventional electron spin resonance is used to measure the nuclear spin transition frequencies of the ^{31}P nuclear spins, where the ^{31}P electron spins are detected electrically via spin-dependent transitions through Si/SiO_2 interface states, thus not relying on a polarization of the electron spin system. In addition, the electrical detection of coherent nuclear spin oscillations is shown, demonstrating the feasibility to electrically read out the spin states of possible nuclear spin qubits.

DOI: 10.1103/PhysRevLett.106.187601 PACS numbers: 76.70.Dx, 03.67.−a, 71.55.Cn, 76.30.−v

Control and readout of electron spin states in solids are well established down to the single spin level [1,2]. In contrast, the readout of nuclear spin states has mostly been limited to optical techniques [3,4]. However, for nanostructures not exhibiting luminescence, an electrical readout scheme is advantageous. Electrical detection of nuclear magnetic resonance has been performed on, e.g., two-dimensional electron gases, identifying the origin of the Overhauser field [5], and the electrical readout of nuclear spin states has been achieved for this system [6]. In phosphorus-doped silicon, McCamey *et al.* [7] have recently demonstrated the electrical readout of nuclear spins at 8.6 T. While both these studies employ highly polarized electron spin systems for the readout [6–9], we make use of a spin-dependent recombination process via Si/SiO_2 interface states [10]; this approach does not rely on a polarization of the electron spin system and thus works under experimental conditions where the thermal energy is much larger than the electron Zeeman splitting [11]. We here demonstrate the electrical detection of coherent nuclear spin oscillations in phosphorus-doped silicon using pulsed electrically detected electron nuclear double resonance (EDENDOR) at 0.3 T using X-band frequencies (10 GHz). Outside the framework of quantum computation, pulsed EDENDOR could become a valuable spectroscopic tool for the characterization of point defects in semiconductors combining the high sensitivity of continuous-wave EDENDOR [12] with the reduction of the dynamic complexity of the coupled electron and nuclear spin systems via pulsed spectroscopy [13].

The principle of pulsed EDENDOR is depicted in Fig. 1. For the ^{31}P donor in silicon to be investigated, its electron spin $^{31}P_e$ ($S = 1/2$), its nuclear spin $^{31}P_n$ ($I = 1/2$), and their hyperfine coupling give rise to a four-level system. For the electrical readout we use a spin-to-charge conversion mechanism based on a spin-dependent recombination involving the ^{31}P donor electron and the P_{b0} center ($S = 1/2$) at the Si/SiO_2 interface [10]. Accounting for the two orientations of the P_{b0} spin, we sketch the eight different states for the three involved spins in panel (i), indicating the occupation of the different states by the gray bars. Because of the Pauli principle, spin pairs with antiparallel spins recombine while the pairs with parallel orientation are long lived. Therefore, in the steady state only levels associated with parallel orientations of $^{31}P_e - P_{b0}$ pairs are occupied [11] with a probability of 1/4 each. We neglect the polarization of the spin system at first.

The presented pulsed EDENDOR experiments are based on the Davies pulse sequence for conventional pulsed electron nuclear double resonance (ENDOR) [14]. At first, we describe the EDENDOR experiments assuming that no

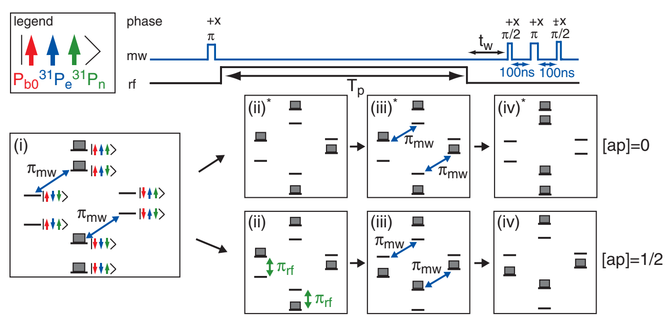

FIG. 1 (color online). The basic pulse sequence of the electrically detected Davies ENDOR consists of a preparation microwave π pulse, an rf pulse of length T_p, and a mw detection π pulse after a waiting time t_w [3]. The evolution of the spin state populations for this sequence is depicted in the panels. The donor electron spin ($^{31}P_e$), its nuclear spin ($^{31}P_n$), and the electron spin of the Si/SiO_2 interface state (P_{b0}) are symbolized by the three arrows in the ket as shown in the legend. The populations of the spin states are indicated by gray boxes. The fraction of antiparallel electron spin pairs at the end of the pulse sequence is given by $[ap]$. We replace the final mw π pulse by a spin echo sequence as discussed in the text.

recombination occurs on the time scale of the pulse sequence. The preparation microwave (mw) π pulse inverts the populations of the levels associated with one of the two $^{31}P_e$ hyperfine transitions (i). Subsequently, a radiofrequency (rf) π pulse inverts the populations on one of the $^{31}P_n$ hyperfine transitions (ii). Since the signal observed in pulsed electrically detected magnetic resonance is proportional to the fraction $[ap]$ of $^{31}P_e$-P_{b0} pairs with antiparallel spins at the end of the pulse sequence [15], a detection mw π pulse is applied to electrically readout the nuclear spin state (iii). At the end of this pulse sequence, we expect an antiparallel spin fraction of $[ap] = 1/2$ when an rf π pulse has been applied (iv) whereas $[ap] = 0$ without an rf pulse or with an rf pulse far off resonance (iv)*. In contrast to conventional ENDOR, where the ENDOR intensity is limited by the polarization of the electron spin ensemble, the EDENDOR intensity is given by $[ap]$, which can be significantly larger.

For the measurements of EDENDOR, we used a sample consisting of a 22 nm-thick Si layer with a nominal P concentration of 9×10^{16} cm^{-3} grown by chemical vapor deposition on a 2.5 μm thick, nominally undoped Si buffer on a silicon-on-insulator substrate. The doped epilayer ensures dominant $^{31}P_e$-P_{b0} recombination [10] while the buried oxide reduces the current flow through the substrate not generating spin-dependent signals. The epilayer is covered with a native oxide. Interdigit Cr/Au contacts with a periodicity of 20 μm defining an active area of 2×2.25 mm^2 were evaporated for photoconductivity measurements. The sample was mounted with the silicon [110] axis parallel to the static magnetic field, illuminated with white light from a tungsten lamp at ≈ 100 mW/cm^2, and biased with 100 mV resulting in a current of ≈ 60 μA. The device forms a metal-semiconductor-metal photodetector and the bias point is chosen in the linear part of the I-V curve to give the best signal-to-noise ratio. All experiments were performed at ≈ 5 K in a BRUKER dielectric microwave resonator for pulsed X-band ENDOR. The microwave-pulse power was adjusted such that the π-pulse length was 30 ns, corresponding to a microwave B_1 field of 0.6 mT. The current transients after the pulse sequence were recorded by measuring the voltage drop over a 1.6 kΩ resistor placed at room temperature in series with the sample. The resulting voltage transients were filtered, amplified, and recorded with a digitizer card. The recorded transients are boxcar integrated [16], resulting in a charge ΔQ that is proportional to the antiparallel spin pair fraction $[ap]$ at the end of the microwave-pulse sequence [15]. The pulse sequence used is shown on the top of Fig. 1. To reduce the background resulting from nonresonant photocurrent transients [17], we replace the final detection mw π pulse by a detection echo sequence [3,18]; by applying a two-step phase cycle [19] to the last microwave $\pi/2$ pulse (indicated in Fig. 1 by $\pm x$), the detection echo sequence forms an effective 2π pulse for $(+x)$ and an effective π pulse for $(-x)$ since a phase change of 180° results in a reversed sense of rotation of the spin states on the Bloch sphere. By changing the phase for every shot and subtracting consecutive traces, only resonant changes in the photocurrent are detected. At a shot-repetition time of 800 μs, which allows the electron spin system to relax to its steady state [18,20], this constitutes a lock-in detection scheme with square-wave modulation at ≈ 660 Hz reducing the noise level in our measurements by at least a factor of 10. To record an EDENDOR spectrum with a signal-to-noise ratio as shown in Fig. 2, the measurement time is typically several hours.

In a first experiment, we demonstrate that pulsed EDENDOR can be used as a spectroscopic method. To this end, we keep the length of the rf pulse fixed at $T_p = 10$ μs while sweeping the rf frequency. Throughout this work, the detection echo sequence with equal evolution times of 100 ns is applied after waiting for $t_w = 2$ μs, cf. Fig. 1. Figure 2(a) shows the integrated current transient ΔQ as a function of the rf frequency f_{rf} for two different magnetic fields, chosen such that the microwave pulses are resonant with the high-field hyperfine-split $^{31}P_e$ resonance (upper trace) and with the P_{b0} centers at $g = 2.0042$ (lower trace) [21]. Both traces show strong variations as a function of the rf frequency, which we attribute to nonresonant effects caused by

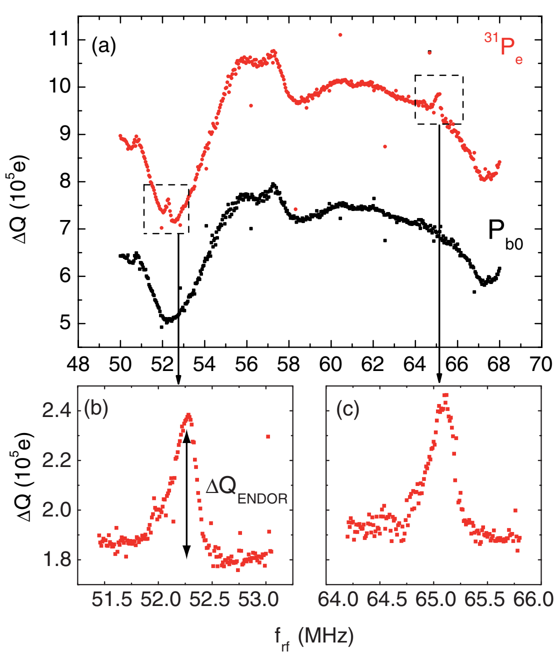

FIG. 2 (color online). (a) Integrated current transient ΔQ after the Davies EDENDOR pulse sequence with $T_p = 10$ μs as a function of the rf frequency. When the mw pulses are in resonance with the $^{31}P_e$ high-field hyperfine line (upper trace) two peaks can be observed at $f_{rf} = 52.25$ MHz and $f_{rf} = 65.08$ MHz. These peaks do not appear in the lower trace where the mw pulses are in resonance with the P_{b0} spins. More detailed frequency scans of the two peaks are shown in panels (b) and (c), where the nonresonant background has been subtracted. ΔQ_{ENDOR} denotes the peak amplitude.

overloading of the voltage amplifier due to the voltage transients induced by the strong rf pulse. Since for nonresonant rf pulses the antiparallel spin content is the same for microwave pulses resonant with the $^{31}P_e$ and with the P_{b0} spins, a comparison of the two traces allows us to identify the $^{31}P_n$ transitions at frequencies of $f_1 = 52.25 \pm 0.02$ MHz and $f_2 = 65.08 \pm 0.02$ MHz. More detailed frequency scans of the two peaks are shown in panels (b) and (c) where the P_{b0} trace was subtracted from the $^{31}P_e$ trace to remove the nonresonant background signal. The measured nuclear transition frequencies are in good agreement with the expected frequencies of 52.34 and 65.19 MHz for the hyperfine interaction of 117.53 MHz between $^{31}P_e$ and $^{31}P_n$, and the $^{31}P_n$ nuclear Larmor frequency of 6.076 MHz [22,23]. The slightly smaller value of the measured frequencies could be attributed to small deviations of the hyperfine interaction at the surface from the bulk value due to local strain in the thin-film silicon sample [24]. To exclude spurious effects of the intense rf pulse (e.g., bolometric), we repeated the same measurement without the preparation mw-π-pulse. As expected, no peaks at the nuclear transition frequencies were observed [16].

To demonstrate the electrical readout of coherent nuclear spin oscillations, we measured the amplitude of the EDENDOR signal as a function of the rf pulse length T_p in a second experiment. To this end, we recorded rf frequency sweeps as those in Fig. 2(b) for different T_p and fitted the peaks with Lorentzians. In Fig. 3, we show their amplitudes $\Delta Q_{\mathrm{ENDOR}}$ as a function of T_p, revealing a damped oscillation. We attribute this oscillation to the coherent driving of the ^{31}P nuclear spins. To corroborate this interpretation, we measured the oscillation period T_{Rabi}, estimated from the position of the first maximum of the oscillation, for different rf power levels P_{rf} resulting in a

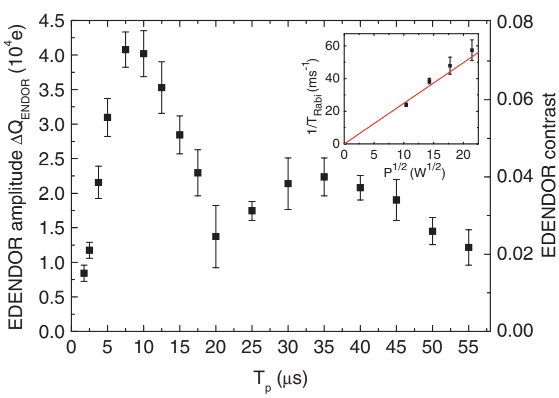

FIG. 3 (color online). Amplitude of the EDENDOR peak $\Delta Q_{\mathrm{ENDOR}}$ at 52.25 MHz as a function of the rf pulse length T_p. The oscillation shows the coherent driving of nuclear spin motion which is damped on the time scale of the recombination of the $^{31}P_e$-P_{b0} spin pairs. The Rabi frequency, estimated from the position of the first maximum of the oscillation, scales linearly with the square root of the rf power, as shown in the inset.

linear increase of the Rabi frequency $1/T_{\mathrm{Rabi}}$ with the rf B_2 field ($B_2 \propto \sqrt{P_{\mathrm{rf}}}$) as shown in the inset of Fig. 3. For longer T_p the oscillation period seems to increase, which might be related to the different time scales of the recombination processes occurring during the rf pulse. To compare the measured EDENDOR amplitude $\Delta Q_{\mathrm{ENDOR}}$ with the theoretically expected maximum value $[ap] = 1/2$ from the considerations depicted in Fig. 1, we take the amplitude ΔQ_{echo} of the detection echo sequence $(-x)$ defined above without preceding mw and rf pulses under the same experimental conditions as a measure for the maximum experimentally achievable value of $[ap]$. We define the EDENDOR contrast as $\Delta Q_{\mathrm{ENDOR}}/\Delta Q_{\mathrm{echo}}$, resulting in a contrast of 0.07 at $T_p = 10\ \mu$s.

The evolution of the spin system during the Davies EDENDOR sequence deviates in several aspects from the ideal situation discussed above. These are primarily the recombination that occurs during the rf pulse and the polarization and relaxation of the electron and nuclear spins. A full simulation of the experimentally observed data will require incorporation of these dynamic effects, e.g., in a system of combined rate equations [15]. To gain a first physical picture, we here separately discuss the effects of the recombination time τ_{ap} characteristic for antiparallel electron spin pairs, of the recombination time τ_p characteristic for the parallel spin pairs, and of the polarization of the nuclear spin system. To independently quantify the recombination time τ_{ap}, we performed an inversion-recovery type of experiment [20]. The observed decay can be described with a stretched exponential $\propto \exp(-(t/\tau_{\mathrm{ap}})^n)$ with $\tau_{\mathrm{ap}} \approx 7\ \mu$s, and $n \approx 0.5$, where τ_{ap} can be varied by several μs by changing the illumination intensity. (The recombination time τ_p is not readily accessible; we assume that it is much longer than τ_{ap} due to the weak spin-orbit coupling in Si and that it is shorter than the shot repetition time used.) Thus, after an rf pulse with a length of $T_p = 10\ \mu$s, we expect an EDENDOR amplitude of $0.3 \cdot \Delta Q_{\mathrm{echo}}$. In addition, the finite excitation bandwidth of the rf pulse only excites about a fraction of 0.3 of the nuclear spin resonance line with a FHWM of 0.24 MHz. This reduces the expected EDENDOR contrast to ≈ 0.1, which agrees well with the observed EDENDOR contrast despite the crude approximations involved.

As Fig. 3 demonstrates, even for times T_p much longer than τ_{ap} we observe an EDENDOR oscillation amplitude. This could at least be qualitatively explained considering the different recombination time scales of parallel and antiparallel spin pairs [16]. Following these considerations and assuming that $\tau_p \gg \tau_{\mathrm{ap}}$, the nuclear spin oscillations are expected to persist for rf pulse lengths $\tau_p > T_p \gg \tau_{\mathrm{ap}}$ making τ_p experimentally accessible by EDENDOR. In analogy to conventional Davies ENDOR [14], the ideal EDENDOR pulse sequence transfers the electron spin polarization to the nuclei. This transfer of polarization allows us to read out the nuclear spin state after waiting times t_w much larger than the recombination times, limited only by T_{1n}. Indeed, we observe an EDENDOR signal for $t_w > 4$ ms with an EDENDOR contrast of 0.01 using a shot-repetition time of 15 ms. This would allow us to measure T_{1n} for donors close to the Si/SiO_2 interface by recording the EDENDOR contrast as a function of t_w.

In conclusion, we have demonstrated the electrical detection of coherent nuclear spin oscillations with pulsed EDENDOR employing Si:P as a model system. Recently, an electrically readable nuclear spin memory with a storage time of 112 s has been demonstrated in Si:P at high magnetic fields (≈ 8 T) using highly polarized electrons [7]. In contrast to this approach, we employ a spin-dependent recombination process via Si/SiO_2 interface states enabling the nuclear spin readout without making use of a polarization of the electron spin system. During the readout process, the electron is removed from the donor, which drastically changes the Hamiltonian describing the spin system. It would be interesting to study the effects of removing and repopulating the electron on the nuclear spin state in detail, e.g., with respect to the relaxation and decoherence of the nuclear spin system. Furthermore, pulsed EDENDOR could give access to the recombination time of parallel spin pairs that has hitherto eluded unambiguous experimental determination as well as the nuclear relaxation time for donors close to the Si/SiO_2 interface. The high sensitivity of the electrical detection of magnetic resonance and the widespread availability of X-band spectrometers makes the presented approach to pulsed EDENDOR an attractive spectroscopic method for the characterization of defects in semiconductor nanostructures. Hereby, hyperfine and superhyperfine interactions can be investigated, which allow us to obtain quantitative information about the electron wave function and the specific environment around the defect. Since it does not rely on polarization of the spin system, this approach could also be particularly attractive for room-temperature EDENDOR spectroscopy, e.g., of endohedral fullerenes such as N@C60 [25].

We thank J. Behrends, K. Lips, A. Schnegg, and A. Stegner for fruitful discussions and for collaboration in performing preliminary experiments at Helmholtz-Zentrum Berlin für Materialien und Energie. The work was supported by DFG (Grant No. SFB 631, C3) and by BMBF (EPR-Solar).

*Corresponding author.
hoehne@wsi.tum.de
†Corresponding author.
dreher@wsi.tum.de

[1] R. Hanson, L. P. Kouwenhoven, J. R. Petta, S. Tarucha, and L. M. K. Vandersypen, Rev. Mod. Phys. **79**, 1217 (2007).
[2] A. Morello *et al.*, Nature (London) **467**, 687 (2010).
[3] F. Jelezko, T. Gaebel, I. Popa, M. Domhan, A. Gruber, and J. Wrachtrup, Phys. Rev. Lett. **93**, 130501 (2004).
[4] L. Childress, M. V. Gurudev Dutt, J. M. Taylor, A. S. Zibrov, F. Jelezko, J. Wrachtrup, P. R. Hemmer, and M. D. Lukin, Science **314**, 281 (2006).
[5] M. Dobers, K. v. Klitzing, J. Schneider, G. Weimann, and K. Ploog, Phys. Rev. Lett. **61**, 1650 (1988).
[6] G. Yusa, K. Muraki, K. Takashina, K. Hashimoto, and Y. Hirayama, Nature (London) **434**, 1001 (2005).
[7] D. R. McCamey, J. V. Tol, G. W. Morley, and C. Boehme, Science **330**, 1652 (2010).
[8] D. D. Thornton and A. Honig, Phys. Rev. Lett. **30**, 909 (1973).
[9] G. W. Morley, D. R. McCamey, H. A. Seipel, L.-C. Brunel, J. van Tol, and C. Boehme, Phys. Rev. Lett. **101**, 207602 (2008).
[10] F. Hoehne, H. Huebl, B. Galler, M. Stutzmann, and M. S. Brandt, Phys. Rev. Lett. **104**, 046402 (2010).
[11] D. Kaplan, I. Solomon, and N. F. Mott, J. Phys. (Paris) **39**, 51 (1978).
[12] B. Stich, S. Greulich-Weber, and J. Spaeth, Appl. Phys. Lett. **68**, 1102 (1996).
[13] C. Gemperle and A. Schweiger, Chem. Rev. **91**, 1481 (1991).
[14] E. Davies, Phys. Lett. A **47**, 1 (1974).
[15] C. Boehme and K. Lips, Phys. Rev. B **68**, 245105 (2003).
[16] See supplemental material at http://link.aps.org/supplemental/10.1103/PhysRevLett.106.187601 for details of the current transient measurement, the data of the control experiment without mw preparation pulse, and the effect of different recombination times ($\tau_p \gg \tau_{ap}$) on the EDENDOR amplitude.
[17] A. R. Stegner, C. Boehme, H. Huebl, M. Stutzmann, K. Lips, and M. S. Brandt, Nature Phys. **2**, 835 (2006).
[18] H. Huebl, F. Hoehne, B. Grolik, A. R. Stegner, M. Stutzmann, and M. S. Brandt, Phys. Rev. Lett. **100**, 177602 (2008).
[19] A. Schweiger and G. Jeschke, *Principles of Pulse Electron Paramagnetic Resonance* (University Press, Oxford, 2001).
[20] S. Y. Paik, S. Y. Lee, W. J. Baker, D. R. McCamey, and C. Boehme, Phys. Rev. B **81**, 075214 (2010).
[21] A. Stesmans, B. Nouwen, and V. V. Afanas'ev, Phys. Rev. B **58**, 15 801 (1998).
[22] G. Feher, Phys. Rev. **114**, 1219 (1959).
[23] M. Steger *et al.*, arXiv:1009.6003v2.
[24] H. Huebl, A. R. Stegner, M. Stutzmann, M. S. Brandt, G. Vogg, F. Bensch, E. Rauls, and U. Gerstmann, Phys. Rev. Lett. **97**, 166402 (2006).
[25] W. Harneit, C. Boehme, S. Schaefer, K. Huebener, K. Fostiropoulos, and K. Lips, Phys. Rev. Lett. **98**, 216601 (2007).